Imaging features of hepatic angiosarcoma: retrospective analysis of two centers

Lei Jiang[1,4,5†], Lijun Xie[2,6†], Zhenheng Wu[1,4,5], Qiming Ke[1,4,5], Mo Chen[1,4,5], Wei Pan[1,4,5], Fuxiu Zhong[1,7], Haijie Hong[1,4,5], Jiangzhi Chen[1,4,5], Xinran Cai[1,4,5], Shun Chen[3], Ling Gan[2,6*] and Yanling Chen[1,4,5*]

Abstract

Purpose Identifying primary hepatic angiosarcoma (PHA) preoperatively is challenging, often relying on post-operative pathology. Invasive biopsy increases bleeding risk, emphasizing the importance of early PHA diagnosis through imaging. However, comprehensive summaries of ultrasound, abdominal computed tomography (CT), magnetic resonance imaging (MRI), and whole- body positron emission tomography-CT (PET-CT) in this context are lacking. This study aimed to investigate the comprehensive imaging characteristics of PHA.

Patients and methods Imaging data were collected from 7 patients diagnosed with PHA via pathology between January 2000 and December 2019 in two provincial grade III hospitals. All patients underwent routine color ultrasound examinations before surgery, with 3 patients receiving contrast-enhanced ultrasound (CEUS).CT scans, both plain and enhanced, were performed on 5 patients, and whole-body PET-CT examinations were conducted on 2 patients.

Results Among the 7 patients with PHA, 4 presented with a single solid intrahepatic mass (2 of which were large), 1 with a single exophytic macroblock type, 1 with a mixed type featuring multiple masses and nodules, and 1 with a multiple nodule type. Conventional ultrasound of PHA showed uneven echoes within the tumor, potentially accompanied by septal zone echoes, and a blood flow grade of 0-I. CEUS displayed early-stage circular high enhancement, a central non-enhancement area, and a "vascular sign" around the tumor. CT scans revealed low-density shadows in the plain scan stage, high peripheral ring enhancement, and punctate nodular enhancement in the arterial phase, with varying intensities and the presence of a "vascular sign." During the portal vein stage, the interior of the tumor was consistently unfilled and exhibited structural disorder. PET-CT showed low-density lesions in the liver and low fluorodeoxyglucose metabolism.

Conclusions Imaging diagnosis plays a crucial role in PHA diagnosis. When liver tumor imaging matches the above characteristics, consider PHA.

Keywords Angiosarcoma, Contrast-enhanced ultrasound, Computed tomography enhancement, Positron emission tomography-computed tomography, Liver tumor

†Lei Jiang and Lijun Xie contributed equally to this work.

*Correspondence:
Ling Gan
linggan_1129@fjmu.edu.cn
Yanling Chen
drchenyl@126.com
Full list of author information is available at the end of the article

Jiang *et al. BMC Cancer*   (2024) 24:1191

Page 2 of 10

Introduction

Primary hepatic angiosarcoma (PHA) is an exceptionally rare malignant mesenchymal tumor marked by high malignancy and a grim prognosis, constituting less than 1% of primary liver tumors [1]. The majority of untreated patients succumbed to the disease within six months. Even with comprehensive treatment primarily focused on surgery, most patients did not survive beyond two years [2]. There has been a continual quest for pathogenic genes potentially unique to sarcomas. One study revealed that about 81% of patients with uterine leiomyosarcoma harbor at least one gene mutation, notably more prevalent in metastatic lesions [3]. However, no significant correlation was observed between mutation and overall survival rates. The impact of adjuvant chemotherapy in preventing early sarcoma recurrence is also not markedly significant [4]. Consequently, current strategies aimed at enhancing the prognosis of sarcoma patients do not evoke optimism.

PHA primarily comprises blood vessels or lymphatic endothelial cells, characterized by an abundance of blood vessels that can result in spontaneous rupture and bleeding. Typically lacking distinct clinical symptoms, signs, and specific serum markers, PHA poses a formidable challenge for preoperative diagnosis, often relying on postoperative pathological examination. Preoperative invasive puncture biopsies increase the risk of intraoperative bleeding, often necessitating emergency surgical intervention for hemostasis [5]. Hence, early diagnosis of PHA through imaging is crucial.

In prior research, we summarized the magnetic resonance imaging (MRI) features of four PHA patients, revealing mixed heterogeneous masses with profoundly disordered vascular structures [6]. Previous investigations into preoperative imaging of PHA have primarily utilized single imaging modalities such as abdominal computed tomography (CT) or MRI [7, 8]. Comprehensive analytical reports covering ultrasound, abdominal CT, MRI, and whole-body positron emission tomography-CT (PET-CT) imaging of PHA are scarce. In this study, we retrospectively analyzed ultrasound, CT, PET-CT, and other imaging data from seven PHA patients at two medical centers to collect a comprehensive characterization of PHA based on imaging findings.

Materials and methods

Patients

Between January 2000 and December 2019, imaging data from 7 patients diagnosed with PHA through pathological confirmation were collected at two provincial-level tertiary hospitals (4 patients at one center and 3 patients at the other). This cohort comprised 4 males and 3 females, with a median age of 52.7 years (range 24 to 63 years). All 7 patients underwent routine color doppler ultrasound examinations of the liver and gallbladder, with 3 of them also undergoing contrast-enhanced ultrasonography. Additionally, both CT plain scans and enhanced examinations were conducted on 5 patients, while whole-body PET-CT examinations were performed on 2 patients. The ultrasound, CT, and PET-CT of both centers have the same equipment. Clinical presentations varied among the patients. Three patients experienced right upper abdominal discomfort, and one patient presented with a sizable abdominal and pelvic tumor due to PHA's downward growth on the liver's surface, compressing the right appendage. Liver tumors were incidentally discovered during routine physical examinations in the remaining 3 patients. Among the personal histories of these patients, only one had a prolonged history of chemical exposure due to employment in a mining company, while no history of exposure was reported by the other patients. Testing for alpha-fetoprotein (AFP), carcino-embryonic antigen (CEA), and hepatitis B surface antigen (HbsAg) was conducted on all 7 patients, yielding negative results. The clinical characteristics of seven patients of PHA are shown in Table 1. Approval for this study was granted by the institutional ethics committee of Fujian Medical University Affiliated Union Hospital, and informed consent was obtained from all participants.

Ultrasound

A Philips IU22 high-end color ultrasound diagnostic instrument was utilized for routine liver and gallbladder color Doppler ultrasound examinations. A convex array probe (C5-1, 1–5 MHz) and SonoVue contrast agent from Bracco in Italy were employed for contrast-enhanced ultrasound (CEUS).

Conventional ultrasound

Prior to the ultrasound examination, patients were instructed to fast for at least 6 h. A standard scan of the right upper abdomen was conducted to evaluate the location, size, internal echo, and vascular supply of the liver tumor. Blood flow signals within the tumor were graded using color doppler flow imaging (CDFI) according to the Adler standard, as follows [5]: Grade 0, indicated the absence of blood flow signal within the tumor; grade I, signified the presence of a small amount of blood flow with 2 internal punctate or rod-shaped blood vessels; grade II, denoted moderate blood flow with 3–4 punctate or rod-shaped blood vessels observed; and grade III indicated massive blood flow, with 5 or more rod-shaped blood vessels or 2 longer blood vessels.

Jiang *et al. BMC Cancer*   (2024) 24:1191

Page 3 of 10

Table 1 The clinical characteristics of sever patients with PHA

Patient	Clinical symptom	Chemical exposure	No. of hepatic mass	Maximum diameter (cm)	Metastases	AFP/CEA/CA19-9	Hepatitis B and C	Conventional ultrasound	CEUS	CT	PET-CT
1	RUA pain	Yes	Single	5.7	No	Negative	Negative	Have	None	None	None
2	None	No	Single	8.8	No	Negative	Negative	Have	None	Have	None
3	None	No	Single	14	No	Negative	Negative	Have	None	Have	None
4	None	No	Single	15	No	Negative	Negative	Have	None	Have	None
5	Ventosity	No	Single	19.8	Yes	Negative	Negative	Have	Have	None	None
6	RUA pain	No	Multiple	2.5	No	Negative	Negative	Have	Have	Have	Have
7	RUA pain	No	Multiple	7	No	Negative	Negative	Have	Have	Have	Have

PHA Primary hepatic angiosarcoma, *M* Male, *F* Female, *RUA* Right upper abdomen, *AFP* A-fetoprotein, *CEA* Carcinoembryonic antigen, *CEUS* Contrast-enhanced ultrasound, *CT* Computed tomography, *PET-CT* Whole-body positron emission tomography-CT

Jiang *et al. BMC Cancer*   (2024) 24:1191

Page 4 of 10

CEUS

The optimal tumor observation section was selected, and the probe was secured in place, entering angiography mode. A suspension of 1.5 mL SonoVue was injected via the middle elbow vein, followed by a rapid injection of 5 mL of normal saline (0.9% NaCl) solution to clear the tubing. Subsequently, we continuously monitored the perfusion and blood flow characteristics of the tumor until the contrast agent completely dissipated, which took a minimum of 5 min. The arterial phase was observed within the first 30 s, the portal vein image was examined between 31 and 120 s, and the delay image was acquired after 120 s. The entire procedure was recorded synchronously, and data analysis was archived.

CT examination

A Siemens 64-slice CT machine was utilized with the following scanning parameters: a tube voltage of 120 kv, tube current of 280 mAs, a slice thickness of 5 mm, and a spacing of 5 mm. During dynamic enhancement, a high-pressure syringe was used to inject the non-ionic contrast agent iohexol at a concentration of 300 mgI/mL through the elbow vein at a rate of 2–3 mL/s. Scanning began after 25–30 s in the dynamic pulse phase, followed by a portal vein scan 60 s later and a delayed scan at 140 s. All dynamic and static image data were stored on the hard disk for backup data analysis.

PET/CT

Perform imaging on a PET/CT scanner (Biograph mCT64, Siemens Medical). The patient fasted for at least 6 h and checked their blood glucose levels (< 200 mg/dl) before injection of [18F]FDG (3.7 MBq/kg). [18F]FDG was purchased from Fujian Andiko Positron Technology Co., Ltd., with a radiochemical purity of over 95%. Collect PET/CT images 1 h after intravenous administration. Low dose plain scanning was performed from the skull to the upper thigh using CARE dose 4D (tube voltage 120 kV, effective tube current 70–120 mA, layer thickness 3.0 mm, rotation time 0.5 min, and pitch index 0.8). Positron emission computed tomography images were collected in 3D mode (matrix 200×200), with 6–8 beds and a scanning time of 2.0 min per person. Use CT data for attenuation correction, iteratively reconstruct all PET data (2 iterations and 21 subsets), and then use specialized software (TURED software, Siemens) to jointly register and display PET/CT images.

Results

Morphological manifestations of PHA

Seven PHA patients were included in this study. Four patients presented with single mass types, two of which were classified as giant mass types, all predominantly

Table 2 Conventional ultrasound and contrast-enhanced ultrasound characteristics of primary hepatic angiosarcoma [number of cases (%)]

Characteristic manifestation	Number of cases
Tumor echo	
Hyperechoic	3 (42.8)
Hypoechoic	4 (57.2)
Isoechoic	0 (0)
Tumor boundary	
Clear	5 (71.4)
Unclear	2 (28.6)
Uniformity of tumor echo	
Even	0 (0)
Uneven	7 (100)
CDFI blood flow signal grading	
Level 0	3 (42.8)
Level 1	3 (42.8)
Level 2	0 (0)
Level 3	1 (14.4)
Enhanced Mode	
Annular	3 (100)
Whole	0 (0)
Enhanced phase	
Faster than liver parenchyma	3 (100)
Synchronous liver parenchyma	0 (0)
Peak intensity	
Above liver parenchyma	2 (66.7)
Equal to liver parenchyma	1 (33.3)
Below liver parenchyma	0 (0)

CDFI Color doplor flow image

located in the right lobe of the liver. The major axis of these tumors measured 5.7 cm, 8.8 cm, 14 cm, and 15 cm, respectively. One patient displayed a unique exogenous single massive tumor that extended along the surface of the right liver into the abdominal and pelvic cavity, encompassing the entire right abdomen and measuring 19.8 cm in its upper and lower diameter. Additionally, one patient exhibited a mixed type of multiple masses and nodules, primarily situated in the right lobe of the liver, with some nodules present in the left lobe, and the main focus had a diameter of approximately 7 cm. Another patient had multiple nodules ranging from 1.5 to 2.5 cm in diameter.

Conventional ultrasound findings

The conventional grayscale ultrasound findings for PHA are summarized in Table 2. Among the seven patients, four displayed hypoechoic masses (Fig. 1A), three exhibited hyperechoic masses, and none of the tumors were isoechoic. In five patients, the tumor boundaries
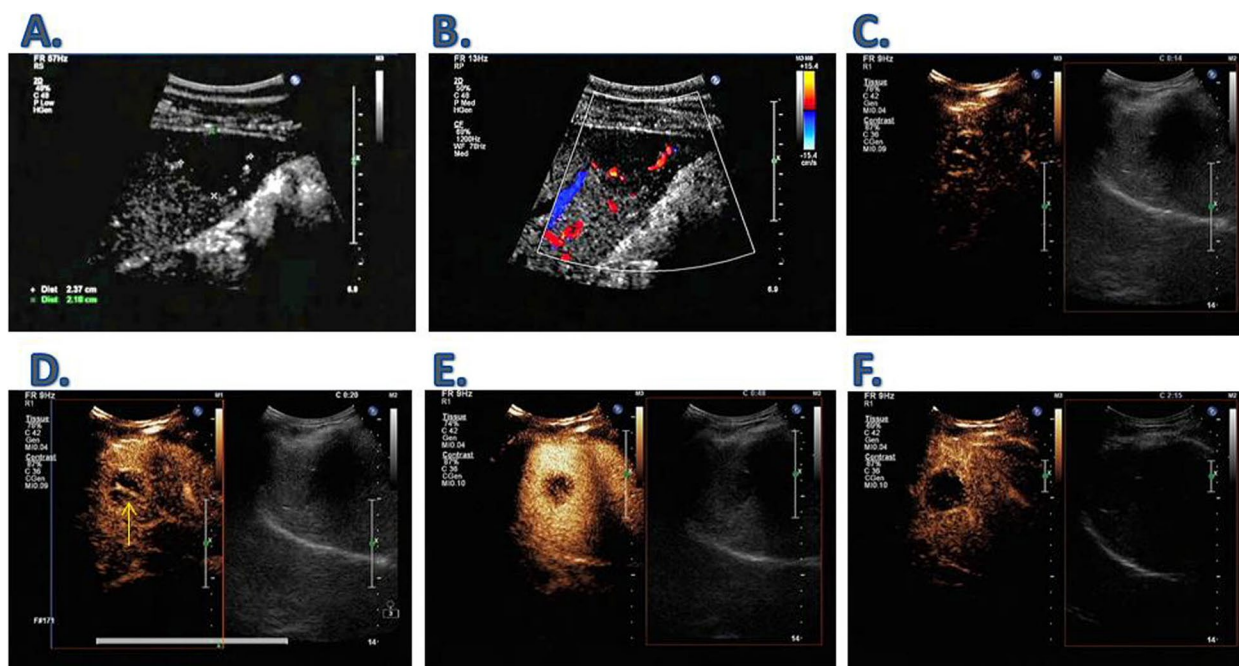
Fig. 1 Ultrasound presentation of primary hepatic angiosarcoma. Patient 6. **A** Conventional ultrasound findings: A hypoechoic mass featuring clear boundaries and uneven internal echoes; **B** Grade I blood flow signal is visible within the tumor; **C** Contrast-enhanced ultrasoundperformance: At 14 s, the lesion exhibited circular enhancement from the periphery, slightly faster than the liver parenchyma; **D** At 20 s, the peak was reached, and a "vascular sign" (yellow arrow) appeared within the circular enhanced lesion, with slightly higher intensity than the surrounding liver parenchyma; **E** The tumor gradually reached its peak within 48 s, but the center remained incompletely filled; **F** During the 135-s delay period, the tumor displayed hypoechoic changes after regression

appeared well-defined (Fig. 1A). Conversely, the remaining two patients featured extensive tumors with indistinct boundaries, and one of them had an exogenous giant tumor extending into the pelvic cavity, reaching the right appendage. In all cases, the internal echo within the tumors was heterogeneous, with multiple septa observed in certain regions (Fig. 2A). The blood flow grading for PHA on ultrasound imaging typically fell within the 0-I range. Three patients displayed no significant blood flow signals within the tumor, while the remaining three had grade I blood flow signals within the tumor (Fig. 1B). In one patient with an exogenous single giant cystic solid tumor, grade III blood flow signals were evident within multiple septa and tumor parenchyma (Fig. 2B). The average value of the blood flow resistance index was 0.48 ± 0.05.

CEUS findings

Among the seven patients, three underwent additional CEUS examinations, as shown in Table 2. Angiography consistently revealed peripheral circular enhancement (Fig. 1C), with a distinct "vascular sign" apparent within the lesion (Fig. 1D) and incomplete filling at the center (Fig. 1E). Notably, one patient had an exogenous single massive cystic solid tumor with pronounced

enhancement of the median septa (Fig. 2C). During the early stage of arterial enhancement, all tumors displayed slightly more rapid enhancement than the liver parenchyma (Fig. 1C). In two patients, the peak intensity of the tumor slightly exceeded that of the surrounding liver parenchyma. In one patient, the peak intensity of the lesion matched that of the surrounding liver parenchyma (Fig. 2E). In both the portal vein phase and the delayed phase, rapid regression and hypoechoic changes were observed within the tumors (Figs. 1F and 2F). Figure 2 illustrates the ultrasonographic findings of a specific case featuring an exogenous single massive PHA.

CT findings

Of the seven patients, five underwent plain and enhanced CT scans. During the plain scan, four patients exhibited low or slightly low-density intrahepatic shadows with well-defined boundaries (Fig. 3A). In the early stages of the arterial-enhanced scan, the tumor showed peripheral circular enhancement, with several punctate nodular enhancements observed within the lesion, characterized by variable intensities and a mixture of these enhancements (Fig. 3B). The peripheral enhancement gradually decreases during the portal phase, while the nodular mixed signals within the lesion are still present (Fig. 3C,
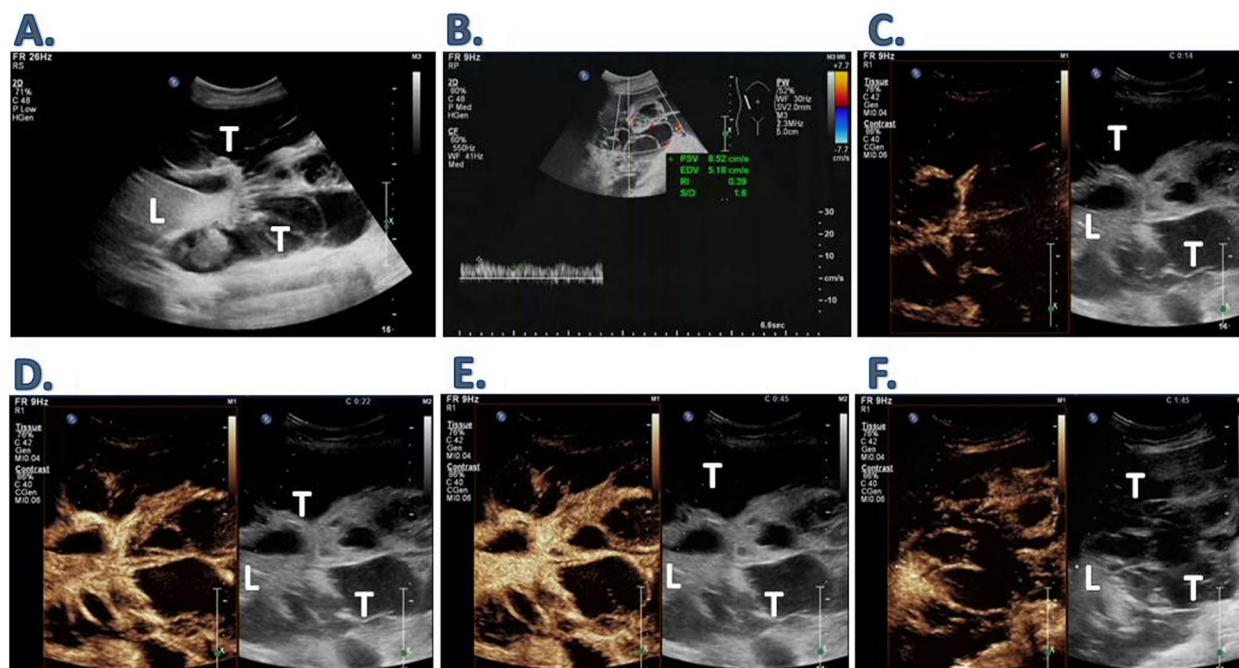
Jiang *et al. BMC Cancer*   (2024) 24:1191

Page 6 of 10

Fig. 2 Ultrasound presentation of a patient with single massive primary hepatic angiosarcoma (congenital type). Patient 5. This figure illustrates a patient with a massive primary hepatic angiosarcoma located on the surface of the liver. The tumor exhibits a cystic and solid structure, growing downwards and compressing the right appendage. **A** and **B** Conventional ultrasound findings: The tumor surrounds the liver's surface, displaying uneven internal ultrasound and unclear boundaries. An interstitial septal pattern is present, with abundant level 3 blood flow signals visible within. The resistance index is 0.39; **C** Contrast-enhanced ultrasound performance: At 14 s, the interstitial septation within the lesion enhanced faster than the liver parenchyma; **D** The peak was reached in 22 s, with the interstitial septation within the lesion exhibiting slightly higher intensity than the liver parenchyma; **E** The cystic part within the tumor compartment remained unfilled at 45 s, and the strength of the interstitial septation equaled that of the liver parenchyma; **F** After 105 s, the intensity of the interstitial septa within the tumor gradually subsided. L: Liver; T: Tumor

D). In one patient, there was a high-density shadow surrounding the mass-type lesion during the plain scan, along with a low-density shadow in the center and indistinct boundaries (Fig. 3E). In the early stages of the arterial-enhanced scan, a mass type gradually became clear in contour as the surrounding ring enhanced, but the interior remained unfilled and structurally disordered (Fig. 3F). In the portal and delayed phases, the lesion's enhancement subsides, but the interior remains unfilled and structurally disordered (Fig. 3G, H). In another patient, Low-density shadows are noticeable during the plain scan, featuring clear boundaries (Fig. 3I). In the early stages of the arterial-enhanced scan, some lesions displayed "vascular signs" (Fig. 3J and K). In the delayed phase, the enhancement within the lesion gradually diminished, although the nodular mixed signal and "vascular sign" remained visible (Fig. 3L).

PET/CT findings

Two PHA patients underwent [18F]FDG PET/CT. The lesions showed low density and low FDG uptake. As shown in Fig. 4, The FDG uptake of the lesion (SUVmax2.8) and liver background (SUVmax2.6) is similar. Tumor to background ratio (TBR) is 1.08.

Discussion

PHA, also known as vascular endothelial sarcoma, Kupffer cell sarcoma, malignant vascular endothelial tumor, among other names, is an exceptionally rare and highly malignant tumor arising from the malignant transformation of hepatic sinus vascular endothelial cells [1]. Its incidence rate is exceedingly low, and it is associated with a dismal prognosis, with the majority of untreated patients succumbing to the disease within six months of diagnosis [9]. Even with treatment, only 3% of patients manage to survive for more than two years [10]. The etiology of PHA remains poorly understood, though some scholars suggest that long-term exposure to chemical substances such as bismuth dioxide colloid, vinyl chloride, and arsenic may be associated with its pathogenesis [11]. In this study, one patient had a prolonged history of chemical exposure due to their employment in a mining company. The clinical presentations of PHA are not distinctive, resembling those of liver cancer, with symptoms such as right upper abdominal pain or incidental

Jiang *et al. BMC Cancer*   (2024) 24:1191

Page 7 of 10

discovery of liver tumors during physical examinations. However, all patients in this study tested negative for serum AFP, CEA, and HBsAg. Consequently, imaging examinations are expected to play a pivotal role in the preoperative diagnosis of PHA, which is the primary objective of this study. Based on tumor morphology, PHA can be categorized into four types: diffuse micronodular, diffuse multinodular, massive, and mixed types. The prevalent types of PHA are diffuse multiple nodules and giant masses [12]. Among the seven patients with PHA in this study, five presented with single giant masses, one had multiple nodules, and one displayed a mixed mass-nodule type.

On conventional grayscale ultrasound, PHA typically presents as having a predominantly low echo with variable boundary clarity [13]. In our study, we observed that among the seven PHA patients, four tumors exhibited hypoechoic characteristics, while three tumors displayed hyperechoic features. Five patients exhibited well-defined tumor boundaries, while two patients had unclear boundaries. Nevertheless, we identified a distinctive pattern in PHA, where the internal echo of the tumor was consistently uneven across all patients, often accompanied by the presence of interstitial septa. Gulmez et al. [14] also reported that one PHA patient displayed uneven echoes on ultrasound, aligning with our study's findings. Concerning CDFI blood flow signals in PHA, they were typically small or entirely absent, falling within grade I or grade II. Only one case presented as a single large cystic-solid tumor with abundant Grade III blood flow signals observed in the internal parenchyma and septum. There are limited literature reports on the CEUS performance of PHA in the existing PubMed database. Trojan et al. [15] conducted CEUS on four PHA patients, reporting that during the arterial and portal phases, three patients exhibited nodular peripheral enhancement, while one patient displayed diffuse chaotic enhancement. During the delayed phase, the tumor center remained incompletely filled. Wang et al. [16] also described a similar CEUS enhancement pattern in a PHA patient, characterized by irregular peripheral marginal enhancement and an absence of central enhancement during arterial and portal phases, with later-stage low enhancement. Articles have discussed CEUS in the differential diagnosis of cystic liver lesions. A significant feature for appropriate differential diagnosis is the low enhancement during the portal vein and sinusoidal phase, with or without arterial enhancement [17]. In particular, CEUS has proven effective in morphological and dynamic evaluations of complex cystic focal liver lesions [18]. In our study, we observed that CEUS consistently showed circular enhancement within all patients, which appeared slightly more intense than the liver parenchyma, with the presence of "vascular signs" in some lesions. The center of the lesion was never fully filled, and in one patient with an exogenous single massive cystic-solid tumor, the median septa exhibited significant enhancement. During the portal vein and delayed phases, tumor enhancement gradually declined. Hence, the annular enhancement surrounding the tumor and the central non-enhancement area may be characteristic features of PHA on CEUS [11]. However, it is essential to note that the absence of enhancement in the central region of the tumor does not necessarily imply tumor necrosis, as it may be associated with the large blood sinuses and reduced blood flow velocity commonly found in PHA [19].

Multiple studies have investigated the utility of CT in diagnosing PHA. Koyama et al. [20] examined 13 PHA patients, noting significant enhancement in both peripheral and central regions during the arterial phase, with incomplete filling of the tumor interior during the portal and delayed phases. They highlighted the diagnostic value of enhanced CT scanning. Similarly, Yi et al. [7] found that CT enhancement of PHA typically exhibited mild enhancement, primarily at the margins, with continuous mild enhancement in the portal vein and delayed phases. Some patients showed "vascular signs". Our study found that most patients displayed low-density shadows with clear boundaries during the plain CT scan phase. In the enhancement phase, circumferential enhancement was evident, along with varied strengths and mixed intensities within punctate nodular enhancements within the lesion. "Vascular signs" were also observed in some lesions, consistent with previous research findings. However, tumors during the portal phase consistently remained unfilled and exhibited structural disorder, resembling CEUS and MRI findings reported earlier [6]. These characteristics included mixed, heterogeneous masses with highly disordered blood vessels. Additionally, we identified punctate nodular enhancement, corresponding to the "arteriovenous short circuit" described by certain scholars [17], was identified.

PET/CT presentations of PHA are rarely documented in the available PubMed database. This study provides a summary of PET/CT observations from two PHA patients, revealing nodular low-density liver shadows. Notably, no significant abnormal FDG hyperactivity was detected within the tumors. However, Zhou et al. [8] reported a unique PHA case in which PET/CT displayed multiple cystic-solid FDG hyperactive tumors in the liver, spleen, abdominal cavity, and retroperitoneal cavity. This study also presents a distinctive case-an exogenous, solitary, massive cystic-solid PHA. The tumor encompasses the liver surface, extending downward towards the right appendage, with an indistinct boundary and disordered interstitial septations. Grade III blood flow signals are
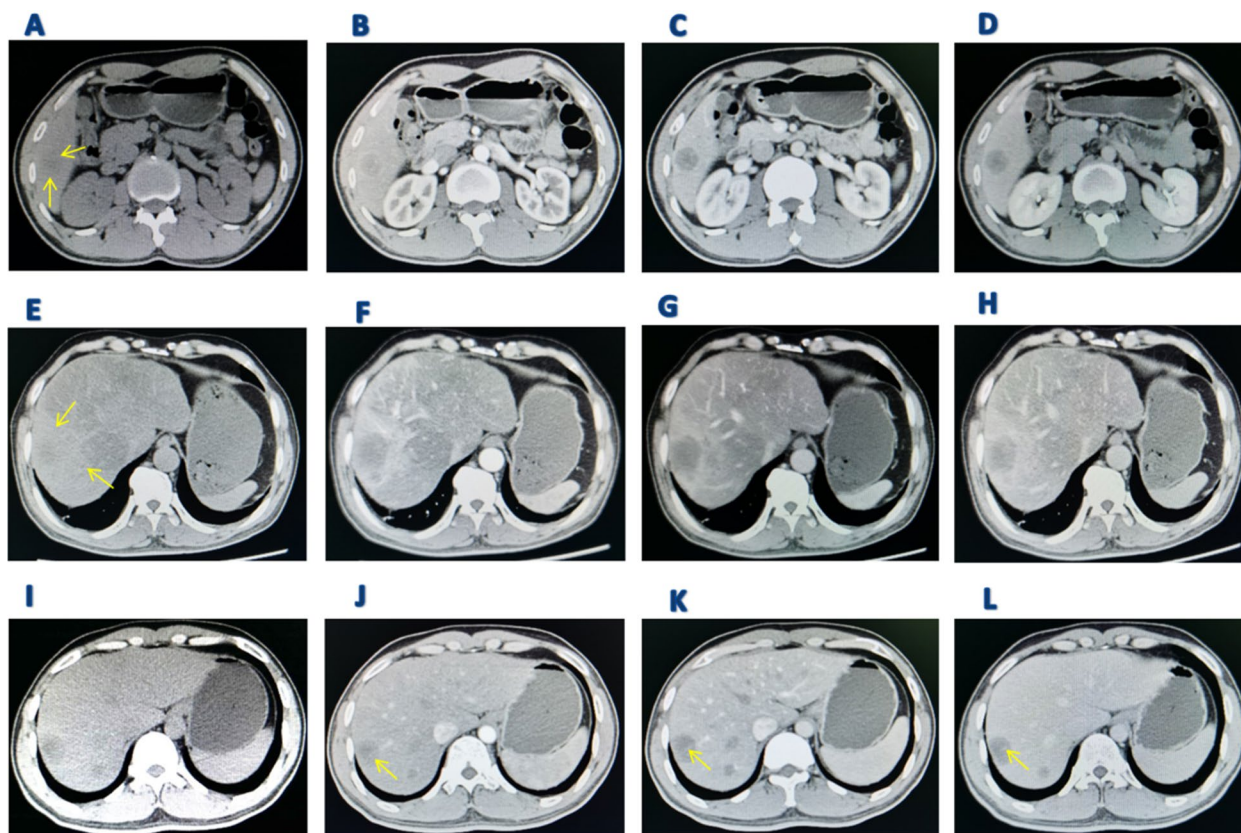
Fig. 3 Computed tomography presentation of primary hepatic angiosarcoma. **A** Patient 6: Low-density shadows are evident during the plain scan, with clear boundaries (yellow arrows); **B** Mild circular enhancement around the arterial phase, along with several punctate nodular enhancements within the lesion, varying in intensity and mixed; **C** and **D** In the portal and delayed phases, peripheral enhancement of the lesion gradually diminishes, while internal nodular mixed signals persist; **E** Patient 7: During the plain scan, peripheral high-density shadows are visible, with low-density shadows at the center and unclear boundaries (yellow arrows); **F** In the arterial phase, the lesion's contour gradually sharpens as the surrounding ring strengthens; **G** and **H** In the portal and delayed phases, the lesion's enhancement subsides, but the interior remains unfilled and structurally disordered; **I** Patient 6: Low-density shadows are noticeable during the plain scan, featuring clear boundaries; **J** Mild peripheral enhancement during the arterial phase, featuring a "vascular sign" (yellow arrow); **K** and **L** In the portal and delayed phases, peripheral enhancement gradually diminishes, yet the "vascular sign" remains visible (yellow arrow)

abundant within the tumor. Regrettably, the patient did not undergo PET/CT examination. We hypothesize that the degree of FDG metabolism may be closely associated with the tumor's internal blood supply. In this particular cohort of two patients, the PET/CT results indicated limited blood supply within the PHA. This hypothesis requires further validation through additional clinical data in the future.

Limitations
While this study provides valuable reference for the imaging diagnosis of PHA, it's crucial to note the limited number of cases included in this project. Further accumulation of case data is necessary to comprehensively outline the typical imaging characteristics of PHA. This study is dual center, retrospective, with a small sample size, and not all patients underwent comprehensive

imaging examinations, so the conclusions drawn are relative. In the coming five years, we anticipate that medical experts specializing in liver diseases globally will collectively concentrate on the imaging manifestations of PHA, aiming to identify commonalities and establish expert consensus.

Conclusion
PHA presents with atypical clinical manifestations, lacks specific serum markers, and is predominantly characterized by solitary giant masses and multiple nodular masses. Notable features of conventional grayscale ultrasound in PHA include uneven echo patterns within the tumor or the presence of interstitial septa, along with minimal or no blood flow signal observed
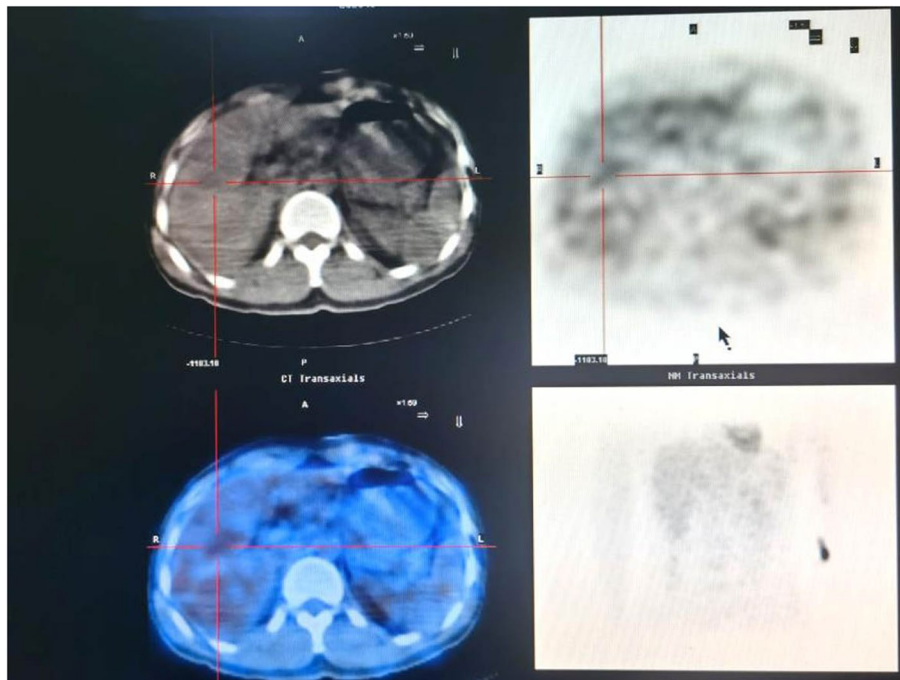
Fig. 4 Positron emission tomography-computed tomography presentation of primary hepatic angiosarcoma. Depiction of low-density liver lesions with low fluorodeoxyglucose metabolism

on color CDFI. CEUS imaging characteristics of PHA encompass circumferential enhancement surrounding the tumor, a central non-enhancing area, and the presence of a "vascular sign". Distinctive CT images of PHA showcase low-density shadows. During the enhancement phase, circular enhancement and "vascular signs" are evident, with punctate nodular enhancements within the lesion, exhibiting variable intensities and mixed characteristics. The interior of the tumor during the portal phase consistently appears unfilled and structurally disordered. Therefore, imaging diagnosis plays a pivotal role in providing essential reference information for the diagnosis of PHA. When liver tumor imaging features align with the descriptions mentioned above, a diagnosis of PHA should be considered.

Abbreviations
PHA Primary hepatic angiosarcoma
CEUS Contrast-enhanced ultrasound
CT Computed tomography
MRI Magnetic resonance imaging

Authors' contributions
Lei Jiang and Lijun Xie conceived and designed the researchs; Lei Jiang, Lijun Xie, Zhenheng Wu, Qiming Ke, Mo Chen, Wei Pan, Haijie Hong, Shun Chen, Xinran Cai, and Lin Gan performed researchs; Lei Jiang, Lijun Xie, Fuxiu Zhong, Jiangzhi Chen, Lin Gan and Yanling Chen analyzed data; Lei Jiang, Lijun Xie, Lin Gan and Yanling Chen wrote the paper. All authors read and approved the final manuscript.

Availability of data and materials
The datasets used and analysed during the current study available from the corresponding author on reasonable request.

Declarations

Ethics approval and consent to participate
This study was approved by the institutional ethics committee of Fujian Medical University Union Hospital. We confirm that all methods are carried out in accordance with the relevant guidelines and regulations of the ethics committee. The patients have signed informed consent in the study.

Consent for publication
Not applicable.

Competing interests
The authors declare no competing interests.

Author details
[1]Department of Hepatobiliary Surgery and Fujian Institute of Hepatobiliary Surgery, Fujian Medical University Cancer Center, Fujian Medical University Union Hospital, Fuzhou 350001, Fujian Province, China. [2]Department of Ultrasonic Image, The First Affiliated Hospital, Fujian Medical University, Fuzhou 350005, Fujian Province, China. [3]Department of Ultrasonic, Fujian Medical University Union Hospital, Fuzhou 350001, Fujian Province, China.

Jiang *et al. BMC Cancer*   (2024) 24:1191

Page 10 of 10

⁴Key Laboratory of The Ministry of Education for Gastrointestinal Cancer, Fujian Medical University, Fuzhou 350108, Fujian Province, China. ⁵Fujian Key Laboratory of Tumor Microbiology, Department of Medical Microbiology, Fujian Medical University, Fuzhou 350108, Fujian Province, China. ⁶Department of Ultrasonic Image, National Regional Medical Center, Binhai Campus of the First Affiliated Hospital, Fujian Medical University, Fuzhou 350212, Fujian Province, China. ⁷Department of Hepatobiliary Surgery Nurse, Fujian Medical University Union Hospital, Fuzhou 350001, Fujian Province, China.

References
1. Molina E, Hernandez A. Clinical manifestations of primary hepatic angiosarcoma. Dig Dis Sci. 2003;48:677–82.
2. Mehrabi A, Kashfi A, Fonouni H, et al. Primary malignant hepatic epithelioid hemangioendothelioma: a comprehensive review of the literature with emphasis on the surgical therapy. Cancer. 2006;107:2108–21.
3. Astolfi A, Nannini M, Indio V, et al. Genomic Database Analysis of Uterine Leiomyosarcoma Mutational Profile. Cancers (Basel). 2020;12(8):2126.
4. Rizzo A, Nannini M, Astolfi A, et al. Impact of Chemotherapy in the Adjuvant Setting of Early Stage Uterine Leiomyosarcoma: A Systematic Review and Updated Meta-Analysis. Cancers (Basel). 2020;12(7):1899.
5. Adler DD, Carson PL, Rubin JM, Quinn-Reid D. Doppler ultrasound color flow imaging in the study of breast cancer: preliminary findings. Ultrasound Med Biol. 1990;16(6):553–9.
6. Jiang L, Xie L, Li G, et al. Clinical characteristics and surgical treatments of primary hepatic angiosarcoma. BMC Gastroenterol. 2021;21:156.
7. Yi LL, Zhang JX, Zhou SG, et al. CT and MRI studies of hepatic angiosarcoma. Clin Radiol. 2019;74(5):406.e1-406.e8.
8. Zhou Z, Lu X, Wang W, Yang J. Hepatic Angiosarcoma With Diffuse Increased 18 F-FDG Uptake on PET/CT. Clin Nucl Med. 2022;47:817–9.
9. Zheng YW, Zhang XW, Zhang JL, et al. Primary hepatic angiosarcoma and potential treatment options. J Gastroenterol Hepatol. 2014;29:906–11.
10 Locker GY, Doroshow JH, Zwelling LA, Chabner BA. The clinical features of hepatic angiosarcoma: a report of four cases and a review of the English literature. Medicine (Baltimore). 1979;58:48–64.
11. Groeschl RT, Miura JT, Oshima K, et al. Does histology predict outcome for malignant vascular tumors of the liver? J Surg Oncol. 2014;109:483–6.
12. Noguchi K, Nakashima O, Nakashima Y, et al. Clinicopathologic study on hepatocellular carcinoma negative for hepatitis B surface antigen and antibody to hepatitis C virus. Int J Mol Med. 2000;6:661–5.
13. Ling W, Qiu T, Ma L, et al. Contrast-enhanced ultrasound in diagnosis of primary hepatic angiosarcoma. J Med Ultrason. 2001;2017(44):267–70.
14. Gulmez AO, Aydin S, Kantarci M. A complementary comment on primary hepatic angiosarcoma: A case report. World J Clin Cases. 2023;11:1814–22.
15. Trojan J, Hammerstingl R, Engels K, et al. Contrast-enhanced ultrasound in the diagnosis of malignant mesenchymal liver tumors. J Clin Ultrasound. 2010;38:227–31.
16. Wang J, Sun LT. Primary hepatic angiosarcoma: A case report. World J Clin Cases. 2022;10:11590–6.
17. Corvino A, Catalano O, Corvino F, et al. Diagnostic performance and confidence of contrast-enhanced ultrasound in the differential diagnosis of cystic and cysticlike liver lesions. AJR Am J Roentgenol. 2017;209:W119–27.
18. Corvino A, Sandomenico F, Setola SV, et al. Morphological and dynamic evaluation of complex cystic focal liver lesions by contrast-enhanced ultrasound: current state of the art. J Ultrasound. 2019;22:251–9.
19. Hanafusa K, Ohashi I, Himeno Y, et al. Hepatic hemangioma: findings with two-phase CT. Radiology. 1995;196:465–9.
20. Koyama T, Fletcher JG, Johnson CD, et al. Primary hepatic angiosarcoma: findings at CT and MR imaging. Radiology. 2002;222:667–73.

Publisher's Note